

# NAD synthase NMNAT acts as a chaperone to protect against neurodegeneration

R. Grace Zhai<sup>1,2,3\*</sup>, Fan Zhang<sup>1\*</sup>, P. Robin Hiesinger<sup>2,†</sup>, Yu Cao<sup>3</sup>, Claire M. Haueter<sup>2</sup> & Hugo J. Bellen<sup>2,3,4</sup>

Neurodegeneration can be triggered by genetic or environmental factors. Although the precise cause is often unknown, many neurodegenerative diseases share common features such as protein aggregation and age dependence. Recent studies in *Drosophila* have uncovered protective effects of NAD synthase nicotinamide mononucleotide adenylyltransferase (NMNAT) against activity-induced neurodegeneration and injury-induced axonal degeneration<sup>1,2</sup>. Here we show that NMNAT overexpression can also protect against spinocerebellar ataxia 1 (SCA1)-induced neurodegeneration, suggesting a general neuroprotective function of NMNAT. It protects against neurodegeneration partly through a proteasome-mediated pathway in a manner similar to heat-shock protein 70 (Hsp70). NMNAT displays chaperone function both in biochemical assays and cultured cells, and it shares significant structural similarity with known chaperones. Furthermore, it is upregulated in the brain upon overexpression of poly-glutamine expanded protein and recruited with the chaperone Hsp70 into protein aggregates. Our results implicate NMNAT as a stress-response protein that acts as a chaperone for neuronal maintenance and protection. Our studies provide an entry point for understanding how normal neurons maintain activity, and offer clues for the common mechanisms underlying different neurodegenerative conditions.

Injury-induced axonal degeneration is dramatically delayed in wallerian degeneration slow (*Wld<sup>S</sup>*) mice, a mutant strain that overexpresses a chimaeric protein containing the NAD synthase NMNAT<sup>3,4</sup>. The *Wld<sup>S</sup>* chimaeric protein offers neuroprotection against axonal degeneration<sup>2,5–7</sup> as well as a variety of neurodegenerative conditions<sup>8–11</sup>. *Wld<sup>S</sup>* protein contains the amino (N)-terminal 70-amino-acid fragment of ubiquitination factor E4B (Ube4b), a unique 18-amino-acid linking region translated from the 5' untranslated region (UTR) of *Nmnat1*, and the entire coding sequence of *Nmnat1*<sup>4,12</sup>. Conflicting results exist in mammalian systems as to whether *Nmnat1* exerts protective effects<sup>13–15</sup> and whether NAD is required<sup>4,14,15</sup>. *Drosophila* contains only one NMNAT gene, whose overexpression delays axonal degeneration<sup>2</sup>. This study and our finding that NMNAT functions as a maintenance factor to protect against activity-induced neurodegeneration<sup>1</sup> suggest that NMNAT alone can protect against multiple neurodegenerative insults. Our recent finding that enzymatically inactive NMNAT retains neuroprotective capabilities also exposed a hitherto unknown molecular function<sup>1</sup>.

To test if NMNAT is a general factor required for neuronal maintenance and protection, we first examined the effects of NMNAT overexpression in a *Drosophila* model for SCA1. Overexpression of wild-type NMNAT or enzyme-inactive NMNAT (NMNAT-WR)<sup>1</sup> suppresses the degenerative phenotypes induced by overexpression of *Drosophila* ataxin-1 (dAtx-1). It also offers moderate protection against the severe phenotypes caused by overexpression of

human ataxin-1 with an expanded (82) poly-glutamine tract (hAtx-1[82Q])<sup>16</sup> (Fig. 1). These findings, and the observations that NMNAT protects from axonal injury<sup>2</sup>, from photoreceptor injury caused by intense light, and that its loss causes massive neurodegeneration<sup>1</sup>, indicate that NMNAT is a versatile neuroprotective agent.

To define the mechanisms of NMNAT function, we turned to a mammalian cell-culture-based assay to evaluate the effect of NMNAT on hAtx-1[82Q] aggregation. When transfected into Cos7

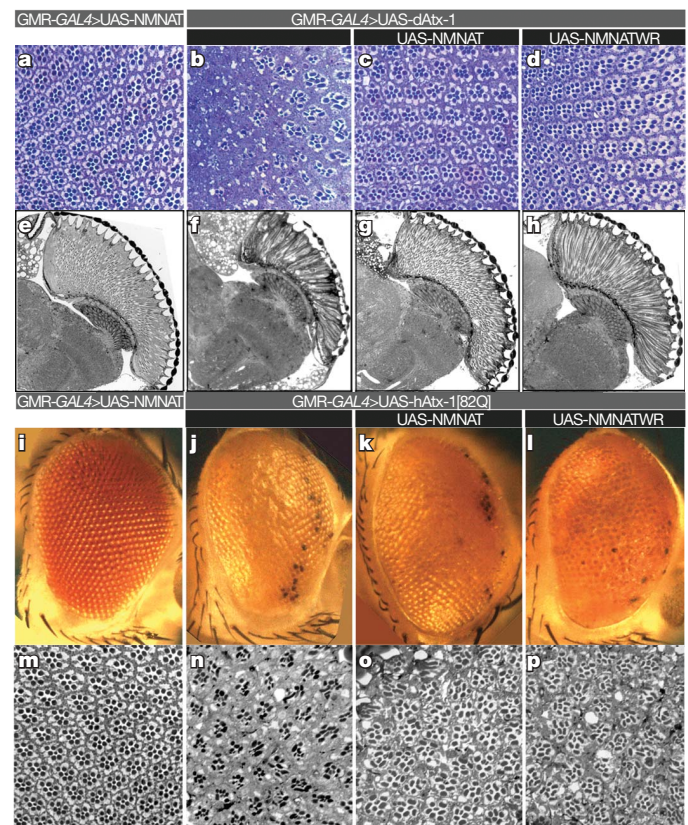


**Figure 1 | NMNAT suppresses toxicity induced by ataxin-1.** **a–h**, Ommatidial morphology of cross section (**a–d**) and horizontal section (**e–h**) of 15-day-old control fly (**a, e**), and flies overexpressing dAtx-1 (**b–d, f–h**). Overexpression of wild-type NMNAT (**c, g**) or enzyme-inactive NMNAT-WR (**d, h**) restores the rhabdomere degeneration phenotype. **i–p**, Eye exterior morphology and ommatidial morphology of two-day-old control fly (**i, m**), and flies overexpressing hAtx-1[82Q] (**j–l, n–p**). Overexpression of hAtx-1[82Q] leads to rough eye (**j**) and reduced rhabdomere size (**n**) phenotypes that are partly suppressed by co-expression of NMNAT (**k, o**) or NMNAT-WR (**l, p**).

<sup>1</sup>Department of Molecular and Cellular Pharmacology, Miller School of Medicine, University of Miami, Miami, Florida 33136, USA. <sup>2</sup>Howard Hughes Medical Institute, Baylor College of Medicine, <sup>3</sup>Department of Molecular and Human Genetics, Baylor College of Medicine, <sup>4</sup>Program in Developmental Biology, Baylor College of Medicine, Houston, Texas 77030, USA. <sup>†</sup>Present address: Department of Physiology and Green Center Division for Systems Biology, University of Texas Southwestern Medical Center at Dallas, Dallas, Texas 75390, USA.

\*These authors contributed equally to this work.

cells, hAtx-1[82Q] forms numerous and often large protein aggregates in both nucleus and cytoplasm<sup>17</sup> (Fig. 2a, b), which are similar to the pathological aggregates found in the neurons of *SCA1* mice or *SCA1* patients<sup>17</sup>. hAtx-1[82Q] appears to be distributed diffusely and/or in aggregated forms in cells (Supplementary Fig. 1A–F). When NMNAT and hAtx-1[82Q] are co-expressed in cells, the percentage of cells with hAtx-1[82Q] aggregates is reduced and more cells contain diffuse hAtx-1[82Q] (Supplementary Fig. 1I). The fluorescence intensity of total hAtx-1[82Q] and its aggregates is significantly reduced (Fig. 2d). This reduction mimics the effect of Hsp70<sup>17</sup> (Fig. 2d), a chaperone known to suppress the pathology associated with hAtx-1[82Q] expression in *SCA1* mice<sup>18</sup>. This similarity between NMNAT and Hsp70 for aggregate formation was further supported when we analysed the solubility of the hAtx-1[82Q] protein by detergent fractionation and high-speed centrifugation. Co-expression of NMNAT or Hsp70 reduced the level in the detergent-insoluble fraction (Fig. 2e, g), arguing that NMNAT, like Hsp70, participates in aggregate reduction. To test whether NMNAT promotes protein degradation through the proteasome-mediated pathway<sup>17</sup>, we impaired the pathway with an inhibitor (MG-132) and evaluated its impact on the protein level of hAtx-1[82Q]. As shown in Fig. 2d, treatment with MG132 increased the total level of hAtx-1[82Q] and aggregates in all cells, including the cells that are co-transfected with NMNAT or Hsp70. Similarly, the level of detergent-insoluble hAtx-1[82Q] is increased in all cells (Fig. 2e, lanes 4–6 compared with lanes 1–3), suggesting that the proteasome is important in controlling aggregate formation. However, the insoluble hAtx-1[82Q] in Hsp70 or NMNAT co-transfected cells is lower than in vector-transfected cells (Fig. 2e, g). This suggests that NMNAT and Hsp70 act only partly through the proteasome to reduce aggregate levels, and that both Hsp70 and NMNAT might also function independently from the proteasome-mediated pathway. Human ataxin-1 without poly-Q expansion (hAtx-1[2Q]) also forms aggregates when expressed in these cells (Supplementary Fig. 1H). This is not surprising, as it has been shown that ataxin proteins without the poly-glutamine expansion also induce neurodegeneration when overexpressed<sup>16</sup>, and overexpression of *Drosophila* ataxin-1 with no poly-glutamine domain induces neurodegeneration (Fig. 1b, f). Importantly, NMNAT is also able to reduce the level of aggregation and the detergent-insoluble fraction of hAtx-1[2Q] (Fig. 2f, h and Supplementary Fig. 1J). These observations suggest that NMNAT reduces the aggregation and promotes the

degradation of ataxin proteins, partly through the proteasome-mediated pathway.

We next examined the *in vivo* response of NMNAT and Hsp70 upon the induction of aggregation of hAtx-1[82Q]. Endogenous NMNAT is located primarily in the cell bodies of most central nervous system neurons<sup>1</sup>, including those of the optic lobes (Fig. 3a). When hAtx-1[82Q] is overexpressed using the pan-neuronal driver *nervana-GAL4*<sup>19</sup>, numerous hAtx-1[82Q] aggregates form in the cell bodies (Fig. 3b, l), similar to cultured cells (Fig. 2). However, unlike in cultured cells, we do not observe diffuse hAtx-1[82Q] localization. Interestingly, endogenous NMNAT is induced and recruited into these aggregates (compare Fig. 3 a, b, f, g). This upregulation and recruitment is very similar to the Hsp70 response when hAtx-1[82Q] is overexpressed (Fig. 3p, q), and expression of dAtx-1 or hAtx-1[82Q] increases the protein level of endogenous NMNAT (Supplementary Fig. 2) and Hsp70.

When NMNAT is overexpressed with *nervana-GAL4*, the protein is not only present in cell bodies, but also in axons (Fig. 3c, h, w). This is consistent with its protective effects in axonal degeneration when overexpressed<sup>2</sup>. To test the effects of hAtx-1[82Q] on the localization of overexpressed NMNAT, we overexpressed both proteins together. NMNAT is recruited into the hAtx-1[82Q] aggregates (see also Fig. 3d, i, n, x) and so is the enzymatically inactive NMNAT-WR (Fig. 3e, j, o, y). The recruitment of NMNAT into hAtx-1[82Q]-induced aggregates is specific, because green fluorescent protein (GFP) is not incorporated into the aggregates when co-expressed (Supplementary Fig. 3). The addition of NMNAT into hAtx-1[82Q] aggregates likely reduces the toxicity associated with hAtx-1[82Q] because the total level of hAtx-1[82Q] is reduced when co-expressing NMNAT or NMNAT-WR (Supplementary Fig. 3E). Taken together, our studies suggest that, in cultured cells, NMNAT functions with the proteasome to reduce the level of aggregation; in the fly brain, NMNAT is recruited into the hAtx-1[82Q] aggregates to reduce the neuronal toxicity induced by hAtx-1[82Q].

In wild-type brains, the level of Hsp70 was below our detection limit (Fig. 3p). However, when hAtx-1[82Q] is overexpressed, Hsp70 expression is strongly induced (compare Fig. 3p, q) and it co-localizes with endogenous NMNAT and hAtx-1[82Q] aggregates (Fig. 3b, q, v). When overexpressed, both enzymatically active and inactive forms of NMNAT are recruited with Hsp70 into hAtx-1[82Q] aggregates (Fig. 3i, j, s, t). These data indicate that NMNAT is upregulated and

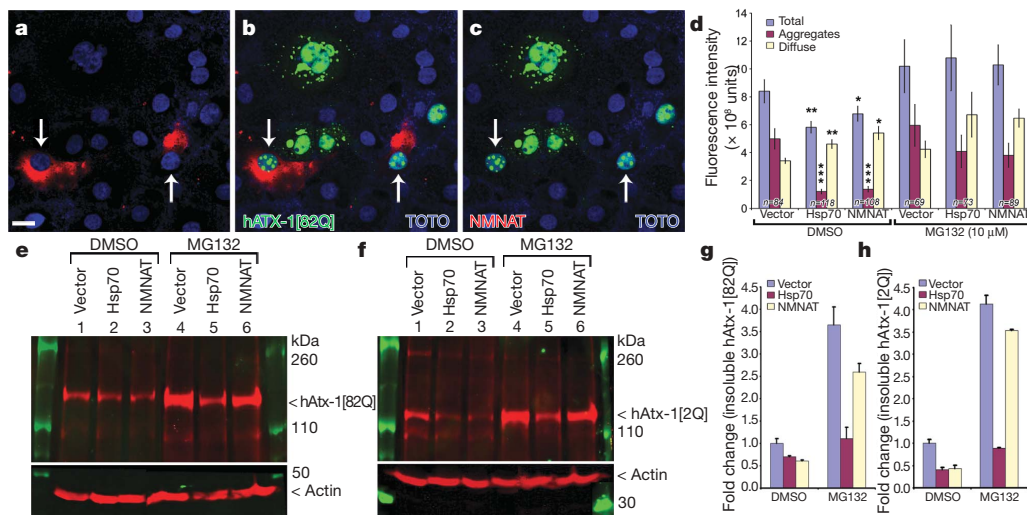


**Figure 2 | NMNAT acts as a chaperone in cultured cells.** a–c, Cos7 cells are co-transfected with hAtx-1[82Q]-GFP (green) and NMNAT (red). TOTO3 staining (blue) marks nuclei. Scale bar in a for a–c, 20  $\mu$ m. d, Quantification of GFP fluorescence. Aggregates are defined as objects at least 0.4  $\mu$ m<sup>2</sup> and 3,600 intensity units. Error bars, s.e.m. \* $P$  < 0.05, \*\* $P$  < 0.01, \*\*\* $P$  < 0.005 (analysis of variance post-hoc test). e–h, Western analysis (e, f) and

quantification (g, h) of detergent-insoluble fractions of cells transfected with hAtx-1[82Q]-GFP (e) or hAtx-1[2Q]-GFP (f) and vector, NMNAT or Hsp70, and treated with either DMSO or 10  $\mu$ M MG132. The level of insoluble hAtx-1[82Q] (g) or hAtx-1[2Q] (h) in the DMSO-treated cells is equal to 1 (fold). Error bars, s.e.m.;  $n$  = 4.

recruited into the hAtx-1[82Q] aggregates in a manner similar to Hsp70, drawing yet another parallel between the function of these two proteins.

Next, we assayed whether NMNAT has chaperone activity. To measure the *in vivo* chaperone activity of NMNAT, we used the assay in which refolding of heat-denatured luciferase is monitored as a measure for chaperone activity<sup>20</sup>. In this assay, heat denaturation, combined with the protein-synthesis inhibitor cycloheximide, renders the endogenous levels of molecular chaperones insufficient to recover luciferase activity fully (Fig. 4a). When we transfect NMNAT as well as its adenylyltransferase-inactive forms (NMNAT-WR and -H30), they all protect luciferase from unfolding during heat shock (red bars in Fig. 4b) and enhance refolding after heat shock (yellow bars in Fig. 4b). In this assay, the chaperone activities of all forms of NMNAT are similar to that of mammalian Hsp70 or *Drosophila* Hsp83, the homologue of mammalian Hsp90<sup>21</sup>. These data indicate that NMNAT protects proteins from unfolding and promotes refolding, either by acting as a chaperone or by regulating the activity of other chaperones.

To distinguish between these possibilities, we used an *in vitro* biochemical assay to measure chaperone activity. This assay measures the chaperone's ability to reduce thermally or chemically induced aggregation of a model protein substrate such as citrate synthase or insulin<sup>22</sup> (Fig. 4c). As shown in Fig. 4e, Hsp70 efficiently reduces thermally induced aggregation of citrate synthase at 43 °C in

the absence of ATP, in a concentration-dependent manner, confirming that it acts as a chaperone<sup>23</sup>. Lysozyme, which has no known chaperone activity, does not effectively suppress thermally induced aggregation of citrate synthase (Fig. 4d). Incubation of citrate synthase with increasing amounts of NMNAT results in a concomitant decrease in citrate synthase aggregation (Fig. 4f). The chaperone activity is quantified by the relative aggregation rate (Fig. 4g), and by the percentage of aggregation reduction at the saturation point (Fig. 4h). The reduction in light scattering (absorbance at 360 nm) is not due to a loss of substrate proteins by degradation, as the levels of citrate synthase remain the same with or without added chaperones (Supplementary Fig. 4). Similar results were obtained with insulin as a model substrate (Fig. 4i), where aggregation of insulin is induced by adding the reducing agent DTT. As in the hAtx-1[82Q] aggregation experiments, enzymatically inactive NMNAT-WR and another inactive NMNAT, NMNAT-H30,<sup>1</sup> are both able to suppress protein aggregation effectively (Fig. 4g, h). This further suggests that the chaperone activity of NMNAT is independent of its NAD synthesis activity. Both wild-type and enzymatically inactive NMNAT efficiently inhibit aggregation in a similar manner to Hsp70, unlike bovine serum albumin (BSA) or lysozyme (Fig. 4i). Note that the human homologue hsNMNAT3 displays chaperone activity similar to the *Drosophila* proteins (Fig. 4b, g, h, i), suggesting that the NMNAT homologues function similarly<sup>1</sup>.

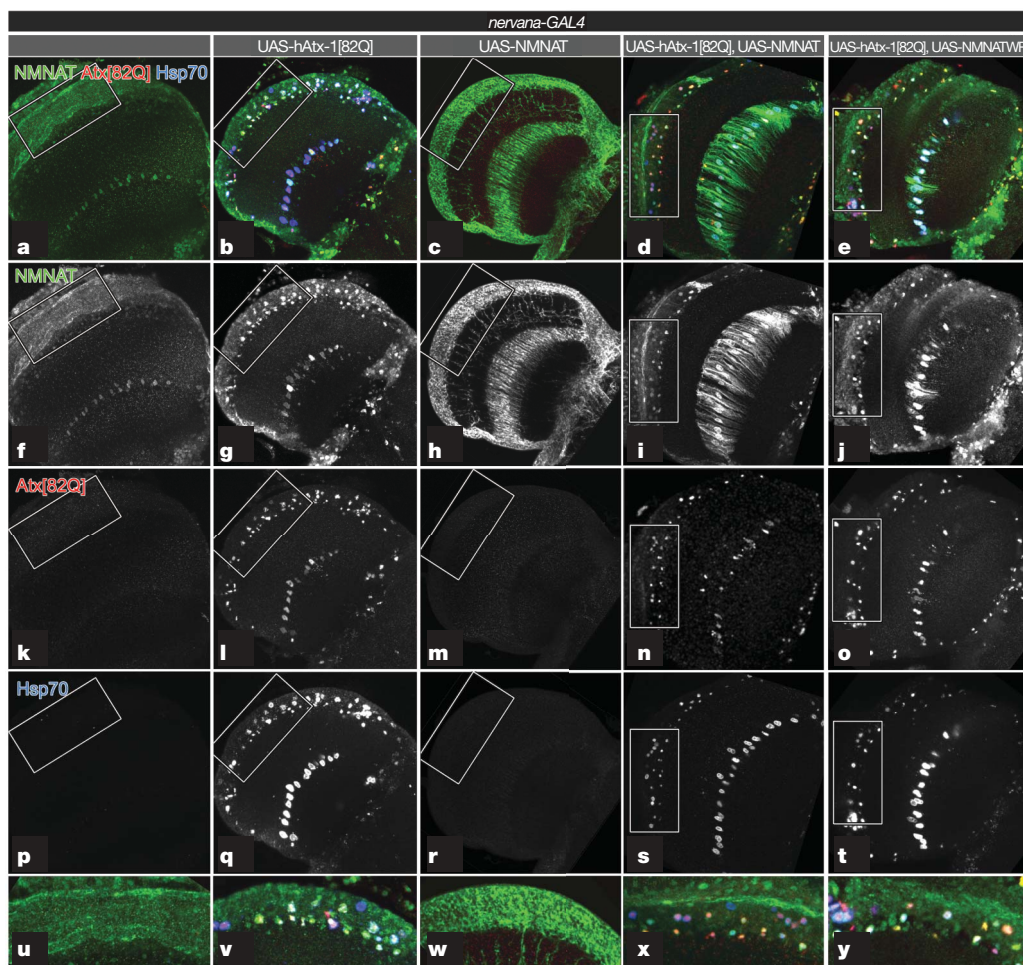


**Figure 3 | Endogenous and overexpressed NMNAT proteins are recruited with Hsp70 into the hAtx-1[82Q] aggregates.** a–e, Seven-day-old adult fly brains were stained for NMNAT (green; f–j), hAtx-1[82Q] (red; k–o) and Hsp70 (blue; p–t). Higher magnifications of boxed areas are shown in u–y. Endogenous NMNAT is primarily nuclear (f). hAtx-1[82Q] forms nuclear aggregates (l). Endogenous NMNAT is upregulated and recruited to

the aggregates (g). NMNAT is distributed to the cytoplasm when singly overexpressed (h), but is recruited to ataxin aggregates when co-expressed with hAtx-1[82Q] (i, n). Enzymatically inactive NMNAT-WR is also recruited into ataxin aggregates when co-overexpressed with hAtx-1[82Q] (j, o). Hsp70 is upregulated and recruited into the aggregates (q, s, t).

If NMNAT has chaperone activity independent of its NAD synthesis ability, there may be a specific domain associated with this function. We therefore created three truncated proteins: NMNAT- $\Delta$ C, deleting the carboxy (C)-terminal domain including the ATP binding motif; NMNAT- $\Delta$ N, deleting the N-terminal catalytic motif; and NMNAT- $\Delta$ CN, deleting both N and C termini (Supplementary Fig. 5A). The N-terminal catalytic motif is not essential for the chaperone activity (Supplementary Fig. 5C); however, the C-terminal domain containing the ATP-binding domain is required, as neither NMNAT- $\Delta$ C nor NMNAT- $\Delta$ CN have chaperone activity (Supplementary Fig. 5B, D). These data provide additional evidence that NMNAT's chaperone and NAD synthesis activities can be dissociated.

To explore further the structural nature of the chaperone function, we searched for primary sequence similarity between NMNAT and known chaperones, but did not find any sequence homology. However, a DALI search<sup>24</sup> using the structural coordinates of NMNAT1 (Protein Data Bank identity code 1KKU) and NMNAT3 (identity code 1NUR)<sup>25</sup> against the entire Protein Data Bank revealed

that both NMNAT1 and NMNAT3 share similarity with chaperone universal stress protein A (UspA; identity code 1JMV)<sup>26</sup>, with a Z score of 5.1, and Hsp100 (identity code 1JBK)<sup>27</sup>, with a Z score of 2.8. A structural superposition of NMNAT1 and UspA showed 13% sequence identity and a root mean squared deviation of 3.0 Å over the entire length of the protein. Hence, NMNAT proteins display structural similarities with known chaperones.

The induction and recruitment of NMNAT upon hAtx-1[82Q] aggregate formation suggest that NMNAT is also a stress-response protein similar to heat-shock proteins. The redistribution of over-expressed NMNAT and co-localization with Hsp70 at intracellular aggregates suggest that NMNAT may act in concert or in parallel with Hsp70. Our data also indicate that NMNAT and Hsp70 act independently, as we observe additive effects when mixing the two proteins in our *in vitro* assay (Supplementary Fig. 6). The chaperone function of NMNAT is likely linked to the proteasome-mediated pathway, as NMNAT is able to reduce the aggregation and promote the degradation of misfolded proteins. The chaperone activity offers an explanation for the broad protective activity of NMNAT in different

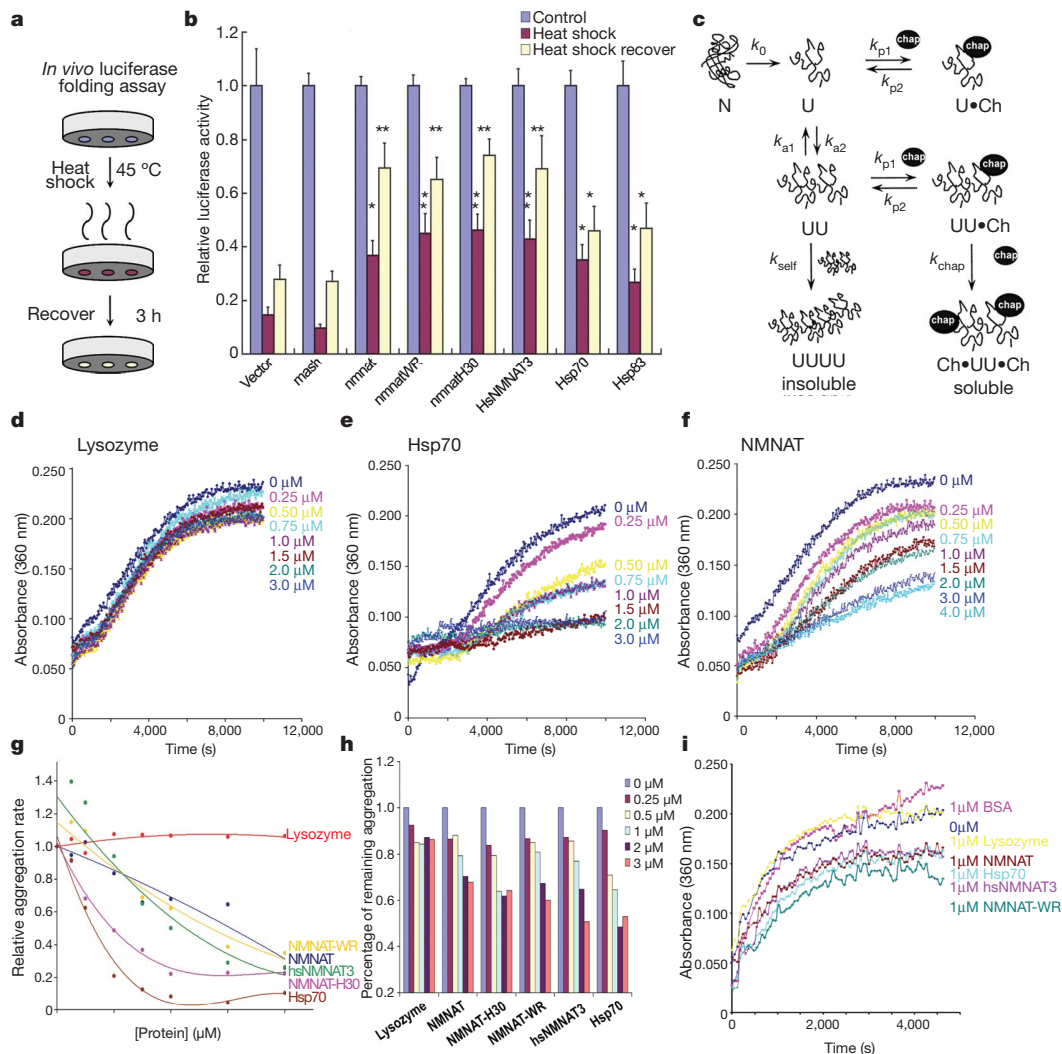


**Figure 4** | *In vivo* and *in vitro* chaperone activity assays. **a**, **b**, Luciferase activity was measured without heat shock as controls (blue columns), after 15 min heat shock at 45 °C (red columns) or after 3 h recovery at room temperature (yellow columns). The luciferase activities relative to the controls are displayed. Error bars, s.e.m. \* $P < 0.05$ , \*\* $P < 0.01$ ; (analysis of variance post-hoc test);  $n = 4$ , triplicate sampling. **c**, Protein aggregation and its inhibition by chaperones. **d–h**, Aggregation of citrate synthase<sup>22</sup> is

prevented by addition of Hsp70 (**e**, **g**), NMNAT (**f**, **g**) or human hsNMNAT3 (**g**) but not by lysozyme (**d**). **g**, The relative aggregation rate is calculated by the change in absorbance per minute and the aggregation rate of CS alone is set to 1. (**h**) The percentage of remaining aggregation is calculated at the saturation point (8000 s). **i**, Insulin aggregation is inhibited by Hsp70, NMNAT, NMNAT-WR or hsNMNAT3 but not BSA or lysozyme.

neurodegenerative conditions. Interestingly, a recent study on the protein–protein interaction network for human inherited ataxias has put NMNAT within the interactome of human ataxin-1<sup>28</sup>.

In summary, our work in *Drosophila* indicates that NMNAT functions as a chaperone independently of its enzymatic activity. Several studies on wallerian degeneration have suggested that the NAD synthesis activity of NMNAT is required for protection of axon degeneration<sup>14,29</sup>. This difference might be partly due to the distinct mechanisms underlying the injury-induced degeneration and other types of neurodegeneration. Further characterization of the role of NMNAT in different degenerative processes will help reveal the mechanisms of neurodegeneration.

## METHODS SUMMARY

The ataxin-1 aggregation assay was performed as described<sup>17</sup> with modifications. Retina sections and transmission electron microscopy were performed as described<sup>1</sup>. Western blot analysis was performed with infrared-dye-conjugated secondary antibodies and imaged on an Odyssey® system (LI-COR Biosciences). The luciferase folding assay was performed as described<sup>21,30</sup>. Confocal microscopy was performed with a Zeiss LSM 510 confocal Axiovert 200M microscope. Fluorescence analysis was performed with MetaMorph 5.07 (Molecular Devices/Universal Imaging Corp.), Amira 3.0 (TGS, Inc.) and Adobe Photoshop 7.0. The aggregation measurements were performed as described<sup>22</sup>. We searched three-dimensional structures on DALI sever<sup>24</sup> (<http://www.ebi.ac.uk/dali/>); the structure superposition was done with PyMol structure analysis software.

**Full Methods** and any associated references are available in the online version of the paper at [www.nature.com/nature](http://www.nature.com/nature).

Received 14 November 2007; accepted 16 January 2008.

Published online 16 March 2008.

- Zhai, R. G. *et al.* *Drosophila* NMNAT maintains neural integrity independent of its NAD synthesis activity. *PLoS Biol.* **4**, e416 (2006).
- MacDonald, J. M. *et al.* The *Drosophila* cell corpse engulfment receptor draper mediates glial clearance of severed axons. *Neuron* **50**, 869–881 (2006).
- Gillingwater, T. H. & Ribchester, R. R. Compartmental neurodegeneration and synaptic plasticity in the *Wld<sup>s</sup>* mutant mouse. *J. Physiol. (Lond.)* **534**, 627–639 (2001).
- Mack, T. G. *et al.* Wallerian degeneration of injured axons and synapses is delayed by a *Ube4b/Nmnat* chimeric gene. *Nature Neurosci.* **4**, 1199–1206 (2001).
- Ribchester, R. R. *et al.* Persistence of neuromuscular junctions after axotomy in mice with slow Wallerian degeneration (*C57BL/Wld<sup>s</sup>*). *Eur. J. Neurosci.* **7**, 1641–1650 (1995).
- Hoopfer, E. D. *et al.* *Wld<sup>s</sup>* protection distinguishes axon degeneration following injury from naturally occurring developmental pruning. *Neuron* **50**, 883–895 (2006).
- Ludwin, S. K. & Bisby, M. A. Delayed wallerian degeneration in the central nervous system of *Ola* mice: an ultrastructural study. *J. Neurol. Sci.* **109**, 140–147 (1992).
- Gillingwater, T. H., Haley, J. E., Ribchester, R. R. & Horsburgh, K. Neuroprotection after transient global cerebral ischemia in *Wld<sup>s</sup>* mutant mice. *J. Cereb. Blood Flow Metab.* **24**, 62–66 (2004).
- Ferri, A., Sanes, J. R., Coleman, M. P., Cunningham, J. M. & Kato, A. C. Inhibiting axon degeneration and synapse loss attenuates apoptosis and disease progression in a mouse model of motoneuron disease. *Curr. Biol.* **13**, 669–673 (2003).
- Samsam, M. *et al.* The *Wld<sup>s</sup>* mutation delays robust loss of motor and sensory axons in a genetic model for myelin-related axonopathy. *J. Neurosci.* **23**, 2833–2839 (2003).
- Sajadi, A., Schneider, B. L. & Aebischer, P. *Wld<sup>s</sup>*-mediated protection of dopaminergic fibers in an animal model of Parkinson disease. *Curr. Biol.* **14**, 326–330 (2004).
- Conforti, L. *et al.* A *Ufd2/D4Cole1e* chimeric protein and overexpression of *Rbp7* in the slow Wallerian degeneration (*Wld<sup>s</sup>*) mouse. *Proc. Natl Acad. Sci. USA* **97**, 11377–11382 (2000).
- Conforti, L. *et al.* NAD<sup>+</sup> and axon degeneration revisited: *Nmnat1* cannot substitute for *Wld<sup>s</sup>* to delay Wallerian degeneration. *Cell Death Differ.* **14**, 116–127 (2007).
- Araki, T., Sasaki, Y. & Milbrandt, J. Increased nuclear NAD biosynthesis and SIRT1 activation prevent axonal degeneration. *Science* **305**, 1010–1013 (2004).
- Wang, J. *et al.* A local mechanism mediates NAD-dependent protection of axon degeneration. *J. Cell Biol.* **170**, 349–355 (2005).
- Tsuda, H. *et al.* The AXH domain of ataxin-1 mediates neurodegeneration through its interaction with Gfi-1/Senseless proteins. *Cell* **122**, 633–644 (2005).
- Cummings, C. J. *et al.* Chaperone suppression of aggregation and altered subcellular proteasome localization imply protein misfolding in SCA1. *Nature Genet.* **19**, 148–154 (1998).
- Cummings, C. J. *et al.* Over-expression of inducible HSP70 chaperone suppresses neuropathology and improves motor function in SCA1 mice. *Hum. Mol. Genet.* **10**, 1511–1518 (2001).
- Sun, B., Xu, P. & Salvaterra, P. M. Dynamic visualization of nervous system in live *Drosophila*. *Proc. Natl Acad. Sci. USA* **96**, 10438–10443 (1999).
- Parsell, D. A., Kowal, A. S., Singer, M. A. & Lindquist, S. Protein disaggregation mediated by heat-shock protein Hsp104. *Nature* **372**, 475–478 (1994).
- Rutherford, S. L. & Lindquist, S. Hsp90 as a capacitor for morphological evolution. *Nature* **396**, 336–342 (1998).
- Chang, Z. *et al.* *Mycobacterium tuberculosis* 16-kDa antigen (Hsp16.3) functions as an oligomeric structure *in vitro* to suppress thermal aggregation. *J. Biol. Chem.* **271**, 7218–7223 (1996).
- Kubo, Y. *et al.* Two distinct mechanisms operate in the reactivation of heat-denatured proteins by the mitochondrial Hsp70/Mdj1p/Yge1p chaperone system. *J. Mol. Biol.* **286**, 447–464 (1999).
- Holm, L. & Sander, C. New structure–novel fold? *Structure* **5**, 165–171 (1997).
- Zhang, X. *et al.* Structural characterization of a human cytosolic NMN/NaMN adenylyltransferase and implication in human NAD biosynthesis. *J. Biol. Chem.* **278**, 13503–13511 (2003).
- Sousa, M. C. & McKay, D. B. Structure of the universal stress protein of *Haemophilus influenzae*. *Structure* **9**, 1135–1141 (2001).
- Li, J. & Sha, B. Crystal structure of the *E. coli* Hsp100 ClpB N-terminal domain. *Structure* **11**, 323–328 (2003).
- Lim, J. *et al.* A protein–protein interaction network for human inherited ataxias and disorders of Purkinje cell degeneration. *Cell* **125**, 801–814 (2006).
- Jia, H. *et al.* Identification of a critical site in *Wld(s)*: essential for *Nmnat* enzyme activity and axon-protective function. *Neurosci. Lett.* **413**, 46–51 (2007).
- Michels, A. A. *et al.* Hsp70 and Hsp40 chaperone activities in the cytoplasm and the nucleus of mammalian cells. *J. Biol. Chem.* **272**, 33283–33289 (1997).

**Supplementary Information** is linked to the online version of the paper at [www.nature.com/nature](http://www.nature.com/nature).

**Acknowledgements** We thank H. Zoghbi and R. Morimoto for reagents. We thank H. Zoghbi, H. Gilbert, H.-C. Lu, X. Zhou, P. Tsoulfas and A. Malhotra for technical suggestions and discussions. We also thank G. McNamara and the Analytical Imaging Core Facility at the University of Miami for imaging assistance. Some confocal imaging was supported by the BCM Mental Retardation and Developmental Disabilities Research Center. R.G.Z., P.R.H., C.M.H. were supported by the HHMI. H.J.B. is an HHMI investigator. R.G.Z. and F.Z. are also supported by the PhRMA Foundation and the Florida Department of Health, James and Esther King Biomedical Research Program.

**Author Contributions** R.G.Z. and H.J.B. conceived the experiments. R.G.Z., P.R.H., Y.C. and C.M.H. performed the genetic and *in vivo* experiments. R.G.Z. and F.Z. performed the *in vitro* experiments. R.G.Z. and H.J.B. wrote the manuscript.

**Author Information** Reprints and permissions information is available at [www.nature.com/reprints](http://www.nature.com/reprints). Correspondence and requests for materials should be addressed to R.G.Z. ([gzhai@med.miami.edu](mailto:gzhai@med.miami.edu)) or H.B. ([hbellen@bcm.edu](mailto:hbellen@bcm.edu)).

## METHODS

**Retina sections and transmission electron microscopy.** Flies of different ages were dissected and fixed at 4 °C in 2% paraformaldehyde, 2% glutaraldehyde, 0.1 M sodium cacodylate, 0.005% CaCl<sub>2</sub> (pH 7.2) and post-fixed in 2% OsO<sub>4</sub>. Thick sections (200 nm) of retina were stained with 1% toluidine blue O, 1% sodium tetraborate (Electron Microscopy Sciences). Thin sections (50 nm) were stained with 4% uranyl acetate and 2.5% lead nitrate. Morphological features were scored double-blind by several observers.

**Ataxin-1 aggregation assay in cultured cells.** The ataxin-1 aggregation assay was performed as described<sup>17</sup> with the following modifications. Briefly, Cos7 cells were doubly transfected with either pEGFP-*hAtx-1[82Q]* and pCMV-*nmnat* or pEGFP-*hAtx-1[82Q]* and pCMV-*hsp70* using Lipofectamine (Invitrogen). After 48 h, cells were fixed and immunolabelled for NMNAT or Hsp70. Cell nuclei were labelled with TOTO3 (Molecular Probes).

**Confocal image acquisition and quantification.** Confocal microscopy was performed with a Zeiss LSM 510 confocal Axiovert 200M microscope equipped with Lasos HeNe 633, HeNe 543, argon ion 488 and Coherent UV Enterprise 351/364 nm laser lines and four identical photomultiplier tubes for blue, green, orange and near infrared fluorescence. Fluorescence analysis was performed with MetaMorph 5.07 (Molecular Devices/Universal Imaging Corp.), Amira 3.0 (TGS, Inc.) and Adobe Photoshop 7.0.

**Protein fractionation and western blot analysis.** To separate proteins into soluble or insoluble extracts, proteins from cultured Cos7 cells were extracted with RIPA buffer (50 mM Tris (pH 8), 150 mM NaCl, 1 mM EDTA, 1% NP40, 0.5% sodium deoxycholate, 0.1% SDS, 1 mM PMSF) and Complete protease inhibitor cocktail (Roche). The detergent-soluble fraction was defined as the supernatant of the cell lysates after centrifugation at 120,000g for 15 min. After removal of the supernatant, the pellets were washed with RIPA buffer and then suspended in 8 M urea, 4% SDS, 0.125 M Tris (pH 6.8), 12 mM EDTA and 3% β-mercaptoethanol. Western blot analysis was performed with infrared dye conjugated secondary antibodies, IR700 and IR800 (LI-COR Biosciences); blots were imaged and processed on an Odyssey® Infrared Imaging system.

**In vivo luciferase folding assay.** The luciferase folding assay was performed as described<sup>21,30</sup>. Briefly, *Drosophila* S2 cells were triply transfected with pAC-*actin-GALA*, pUAST-*luciferase* and one of the following plasmids: pUAST vector, pUAST-*Mash1*, pUAST-*nmnat*, pUAST-*nmnat-WR*, pUAST-*nmnat-H30A*, pUAST-*hsAT3*, pUAST-*hsp70* or pUAST-*hsp83*. At 24 h after transfection, the protein synthesis inhibitor cycloheximide was added and cells were subjected to a 15 min heat shock in an air incubator at 45 °C (which induced efficient unfolding of luciferase without killing the cells) and then allowed to recover at room temperature. Luciferase activity was measured with the Luciferase Assay System (Promega).

**Aggregation measurements.** Aggregation measurements were done as described<sup>22</sup>. Briefly, substrate proteins citrate synthase (Sigma) or insulin (Sigma) were mixed with either BSA (Sigma), egg white lysozyme (Sigma) or affinity-purified recombinant NMNAT, NMNAT-WR, NMNAT-H30, hsNMNAT3 or Hsp70 proteins in HEPES (pH 7.4) buffer. The aggregation of denatured citrate synthase was induced by incubation at 43 °C. The aggregation of insulin was induced by adding reducing agent DTT. Aggregation was monitored by measuring the apparent absorption at 360 nm, because of the Rayleigh scattering of citrate synthase or insulin homo-aggregates versus time. We used a FluoStar Optima plate reader (BMG Labtech) for measurements. The relative chaperone activity of NMNAT was calculated as the scattering of citrate synthase aggregates with time versus NMNAT concentration.

**Immunocytochemistry of fly brains.** Adult brains were fixed in PBS with 3.5% formaldehyde for 15 min and washed in PBS with 0.4% Triton X-100. We used the following antibody dilutions: NMNAT 1:1000; ataxin (gift from Huda Zoghbi, and from NeuroMabs Facility): 1:700; and secondary antibodies conjugated to Cy3, Cy5 or Alexa 488 (Jackson ImmunoResearch; Molecular Probes) were used at 1:250. All antibodies were incubated at 4 °C overnight in the presence of 5% normal goat serum.

**Three-dimensional structure alignment.** The search for similar protein structure was done on DALI sever<sup>24</sup> (<http://www.ebi.ac.uk/dali/>). The three-dimensional structure superposition was done with PyMol structure analysis software.